Research Article

Li-Ting Huang, Yuan-Chieh Cheng, Chung-Yen Wang and Pei-Jen Wang*

Wavefront measurement of plastic lenses for mobile-phone applications

Abstract: In camera lenses for mobile-phone applications, all lens elements have been designed with aspheric surfaces because of the requirements in minimal total track length of the lenses. Due to the diffraction-limited optics design with precision assembly procedures, element inspection and lens performance measurement have become cumbersome in the production of mobile-phone cameras. Recently, wavefront measurements based on Shack-Hartmann sensors have been successfully implemented on injection-molded plastic lens with aspheric surfaces. However, the applications of wavefront measurement on small-sized plastic lenses have yet to be studied both theoretically and experimentally. In this paper, both an in-house-built and a commercial wavefront measurement system configured on two optics structures have been investigated with measurement of wavefront aberrations on two lens elements from a mobile-phone camera. First, the wet-cell method has been employed for verifications of aberrations due to residual birefringence in an injection-molded lens. Then, two lens elements of a mobile-phone camera with large positive and negative power have been measured with aberrations expressed in Zernike polynomial to illustrate the effectiveness in wavefront measurement for troubleshooting defects in optical performance.

Keywords: mobile-phone camera; Shack-Hartmann sensors; wavefront measurements.

*Corresponding author: Pei-Jen Wang, Department of Power Mechanical Engineering, National Tsing Hua University, 101, Sec. 2, Guangfu Road, Hsinchu 30013, Taiwan, Republic of China, e-mail: pjwang@pme.nthu.edu.tw
Li-Ting Huang, Yuan-Chieh Cheng and Chung-Yen Wang: Department of Power Mechanical Engineering, National Tsing Hua University, 101, Sec. 2, Guangfu Road, Hsinchu 30013, Taiwan, Republic of China

OCIS codes: (220.0220) optical design and fabrication; (230.0230) optical devices; (080.0080) geometric optics.

1 Introduction

Optical lenses are crucial in the performance of optical instruments employed for various scientific and industrial applications. Today, many optical lenses for consumer devices are made of plastics and mass produced at low cost by using injection-molding processes. Meanwhile, in the injection-molding process, some technical difficulties, such as geometric deformation, stress-induced birefringence, and refractive index inhomogeneity, are still challenging lens designers and manufacturers. This is mainly due to the complex thermos-mechanical history of plastic lenses experienced throughout the heating, injecting, and cooling stages of the injection-molding processes. As the requirements for compactness and light weight become stringent, the manufacture of minimal total track length (TTL) in mobile-phone cameras is getting more attention in the industry than before. To achieve the minimal TTL goal, optics engineers start adopting highly aspheric surfaces on lens elements and thinner lenses in mobile-phone cameras [1]. Based on the descriptions in published world patents [2], two groups of elements, namely in positive or negative optical power, are commonly employed in the design. They are used for receiving light rays and converging onto the image sensor with chromatic compensation. Therefore, new optical instruments must be designed and studied in order to fulfill efficient on-line inspection of lens elements before the complete module is assembled.

Because modern high-resolution mobile-phone cameras are diffraction limited due to the size of the sensor pixels, performance measurements of aspheric lenses in camera modules are painfully done on various aspheric element designs compared to the spherical elements in large-format cameras [3]. Therefore, it is of great interest to explore the potential of wavefront measurement technology in order to assess or reverse engineer the aspheric design parameters so that the optical qualities of lens

modules can be improved. In the literature, Michaeli et al. reported a straightforward instrument setup in wavefront measurement by using fiber-optic diode laser serving as a point light source and calculated the point spread function (PSF) and modulation transfer function (MTF) of injection-molded and compression-molded plane-convex lenses in 2007 [4]. Later in 2011, Yang et al. first employed wavefront measurement data to study the effects of various packing pressures on the refractive index variations in plastic lenses via the popularly known wet-cell method [5]. Then, Li et al. used numerical simulations based on the finite-element method (FEM) to predict the aberrations based on wavefront data of the lenses of eyeglasses injection molded with polymethyl methacrylate (PMMA) plastics [6]. From the literature review, it is interesting to note that all the papers reported studies of wavefront measurement of plastic lenses in medium or large size with a long focus length. The rationale is concluded as the wavefront measurement in large-format lens elements is technically achievable than the aspheric elements in high-resolution mobile-phone cameras because of the very short focus length and small effective aperture.

In aspheric wavefront measurement with spherical aberration, the most popular methods are based on two fundamental approaches; one uses interferometry measurement adopted from the standard flat and spherical surface testing, while the other is to employ a Shack-Hartmann sensor (SHS) with lens array in front of image capture devices to record the aberrations data in aspheric wavefronts. All wavefront aberrations from the above methods are then processed by computer programs into either an interferogram or polynomial coefficients afterwards. The various testing configurations and relevant algorithms are described elsewhere in the literature [7–9]. However, the interferometry-based testing methods are typically only suitable for specific aspheric surfaces and restricted by the conditions of temporal and spatial coherent light sources. In 2009, Merola et al. reported a self-patterning polydimethylsiloxane (PDMS) micro lens-array characterized by a digital holography method [10]. Of course, the method is still based on interferometers and still sensitive to environmental disturbances, namely air flow, temperature rise, and qualities of laser. On the contrary, an SHS is a device that uses the fact that light travels in a straight line to measure the wavefront of light. A transmissive optics test instrument can be simply constructed with four subunits, namely light source, test object, resizing optics, and wavefront sensor [11]. Today, only a handful of commercial wavefront measurement instruments are available for tests of optical systems exhibiting high-order aspheric aberrations, and they are mostly custom-made with bundled post-analysis numerical programs [12].

2 Measurement of wavefront and aberrations

A wavefront is the locus of points characterized by propagation of position of the same phase. Along a collimated light source, wavefront propagates as a flat surface in the direction of light travel. If the wavefront enters a perfect optical system without aberration, it would be mapped to a perfect spherical wave and converge on the ideal image location, which is named the 'aberration free point'. In a practical optical system, the wavefront deforms in the exit pupil or misses the ideal image point, which is defined by wave aberration function W with optical length measured along a ray from the actual wavefront to the ideal wavefront. Aberrations are imperfections in image formation of optical systems. Some of them are the results of tolerance balancing during design, whereas others are intrinsic to a particular image formation system or the fabrication process of the lenses [13].

The SHS for wavefront measurement consists of a lens array and a charge couple device (CCD) detector. When a wavefront enters the lens array, a focused spot field is captured by the CCD. The snapshot of the focused spot is then analyzed for intensity and location to calculate the wavefront map. A wavefront measurement system based on the SHS can be categorized into four basic configurations, namely basic infinite, finite, infinite, and reflection mode as shown in Figure 1. In the basic infinite setup, the lens under test (LUT) is illuminated by a collimated laser source on one side and measured with SHS by an adjustable telescope tuned at the confocal point for image-size
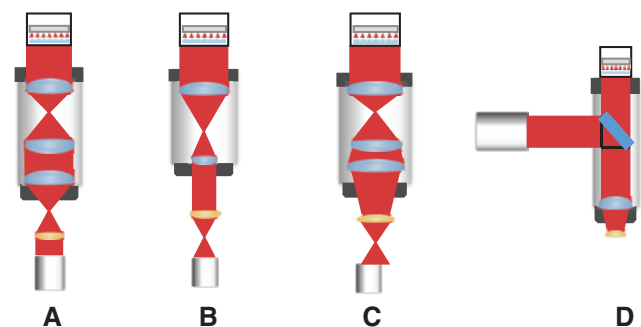

Figure 1: Basic configurations of wavefront measurement with the SHS located at the top and LUT (brown) at the bottom: (A) basic infinite, (B) reverse infinite, (C) finite setup, and (D) reflection mode.

adjustment. This configuration can easily align and locate the focal point of LUT within the mechanical limits. In the reverse infinite setup, the LUT is illuminated with a point laser source emerging from an objective lens; the adjustment of LUT position would re-collimate the point source to a telescope for image-size adjustment. This setup is the most appropriate one for LUT with a short focal length. However, it should be noted that collimating the point light source by the LUT with large aberrations is difficult. The finite setup is a modified version of the reverse infinite configuration. The telescope has been fitted with an extra collimating lens to emulate LUT under application conditions; hereby, the step to adjust the LUT at confocal point is not necessary. The setup provides comfortable adjustment of the LUT position at the best focus point regardless of the LUT characteristics. For optical lenses or reflective surfaces with zero optical power, the reflection setup uses a beam splitter to shorten the optical length without a collimator and give direct wavefront measurements. The above-mentioned four configurations have to be dedicated for LUT based on its optical properties and research objectives.

In injection-molded plastic lenses, the wavefront aberrations are mainly attributed to three original sources, namely refractive index variations, residual birefringence, and geometric surface deviations. To observe materials variations after the process, the wet-cell method is adopted by immersing LUT in lens refractive index matched fluids via a mixture of mineral oils for specific indices. When the LUT is in the wet cell, the wavefront aberrations could only be given by the material refractive index variations plus residual birefringence, as shown in Figure 2. As a
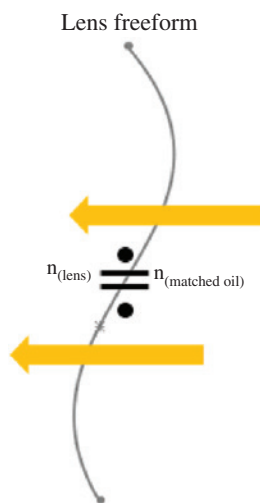
result, the final wavefront errors could be measured by the wavefront measurement system accordingly to assess surface deviations, residual birefringence, and refractive index variations in troubleshooting or product verification processes [14].

3 Experimental setup and procedures

For experimental verification of the theoretical prediction of injection-molded lenses, a plano-convex plastic lens designed with a long focal length was molded with ZEONEX 480R optic polymers. The lens has maximum thickness of 1.125 mm with focal length of 130 mm. The effective aperture radius is 5 mm. Figure 3 illustrates the schematic configuration of the in-house-built instrument based on the basic infinite setup, whereas the wet-cell method and normal wavefront measurements could be conducted for the plano-convex lenses. An He-Ne 5-mW gas laser with wavelength at 543 nm serves as light source connected with a spatial filter and collimator to give a plane wave with measured peal-valley (P-V) and root-mean-square (RMS) basis values in 0.193 and 0.033 waves recorded at the SHS. An iris was used to adjust the beam size to illuminate the LUT in 10 mm diameter. Then, a telescopic lens was placed after the LUT on confocal location to resize the wavefront into the SHS. This configuration is suitable for measurement of aspheric aberrations of LUTs with a long focus length. Moreover, the wet-cell measurement illustrates wavefront aberrations introduced by residual birefringence and refractive index variations. To complete the prediction of residual birefringence via computer aided engineering (CAE) mold-flow simulations, it would be necessary to convert the predicted birefringence into an optic simulation program for wavefront simulations. Figure 4 shows the schematic structure established by the ASAP optics analysis program, copyrighted by BRO, AZ, USA. ASAP can simulate focused spot images and export the image file to wavefront aberrations postprocessing programs. Finally, the simulated wavefront maps are employed as the reference for the verification of measured wavefront maps given by the experiments.

In the experimental cases of plano-convex lens, the predicted results agree well with the experimental measurements. As a further
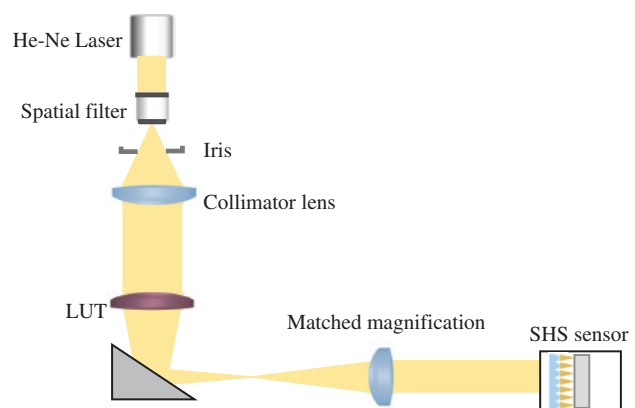

Figure 2: Schematic drawing for the wet-cell method indicating inhomogeneity in lens materials.

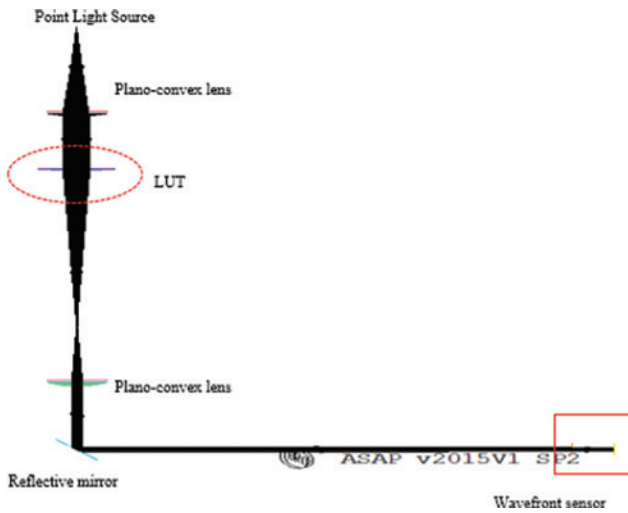**Figure 3:** Schematic configuration of the in-house-built instrument.

Figure 4: Schematics in ASAP simulation of the in-house-built wavefront measurement system.

step, it is of our interest to verify the same approach on the lens elements of mobile-phone cameras. As the lens elements must have a short focal length in a few millimeters, the reverse infinite setup as shown in Figure 5 would be the most appropriate instrument structure. Hence, a wavefront measurement system (model: WaveMaster Pro; Trioptics Inc., Germany) was employed for this part of study [12]. In the study, only two representative elements were measured and

compared to the simulated results because CAE mold-flow simulations are usually time consuming, and two elements should suffice for comparison purposes.

4 Measurement results and discussions

First, the plano-convex plastic lenses were employed for comparisons of wavefront aberrations due to material inhomogeneity and surface deviations between the predicted and measured results. Figure 6 shows the comparisons of wavefront map plots for the plano-convex LUT. The ASAP-simulated ideal wavefront plot is shown at the left-hand side with symmetric characteristics, while the measured plots indicate an anti-symmetric bent-up trend at the left and right edges. Based on the CAE mold-flow simulation results, it is noted that the maximum shear stresses appear at the left and right edges of the LUT, as shown in Figure 7. According to the stress-optical law in photo-elasticity, the refractive index variation is proportional to the shear stress level, which evidently corresponds to the increases in wavefront aberrations at the left and right edges of the LUT. These results agree well with the data reported by Higashihara and Ueda [15]. As a further step to
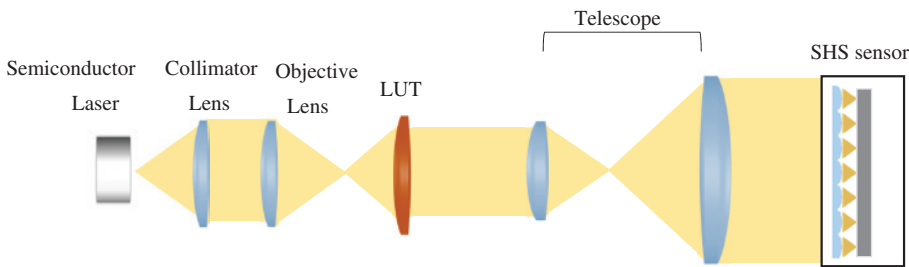

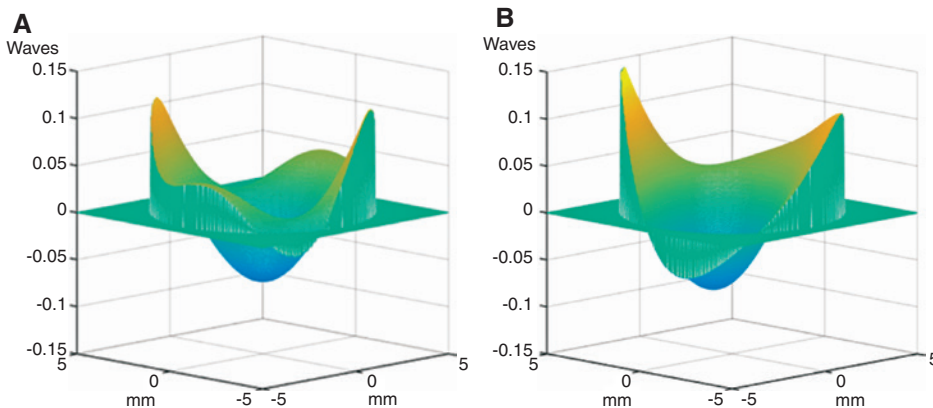**Figure 5:** Schematic layout of the Trioptics WaveMaster Pro instrument.

Figure 6: Comparisons of three-dimensional wavefront plots between the simulated lens design (A) and measured value (B). (A) P-V value=0.213λ and RMS value=0.037λ (B) P-V value=0.232λ and RMS value=0.043λ.
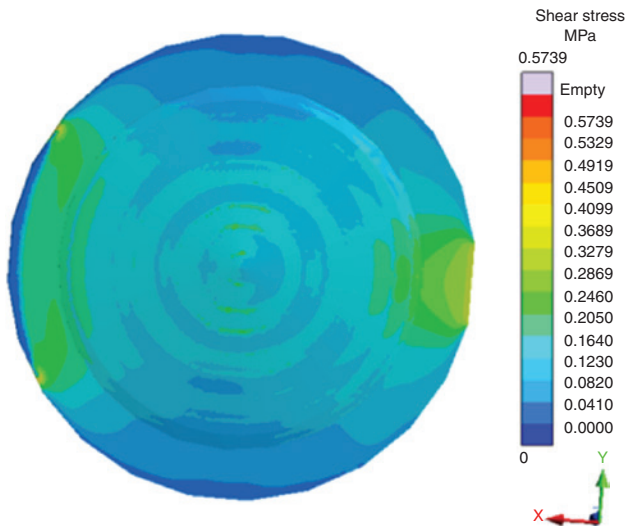
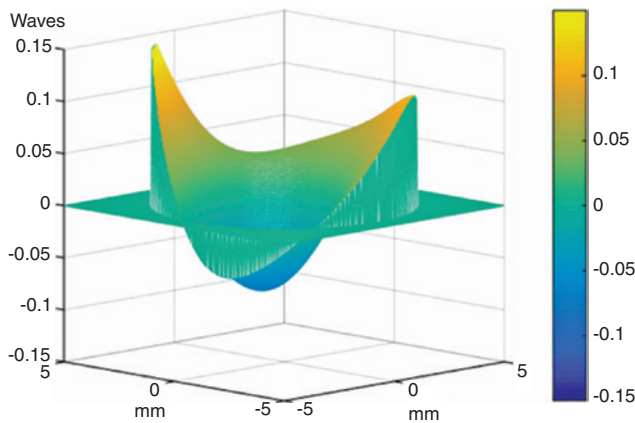**Figure 7:** Plots of shear-stress map based on CAE mold-flow simulation results.

Figure 8: Three-dimensional plots of true measured wavefront aberrations after subtraction of the wet-cell measured value.

explore the above observation, the wet-cell method is conducted for the same LUT. By subtraction of the measured value by the wet-cell method from the directly measured wavefront value, the true wavefront aberrations due to surface deviations of the LUT are plotted in Figure 8. The plot indicates that the minimum peak value and concave feature agree well to the plot of simulated wavefront errors in Figure 6. Hence, it is concluded that wavefront aberrations contributed by residual birefringence and refractive index variations could be experimentally separated from geometric deviations of the surfaces by using the proposed wavefront measurement system.

Finally, it would again be interesting to investigate whether the previous conclusion could be applied for lens elements in mobile-phone cameras with a small back focal length. Taking the first two elements as a comparison study, one of them is an aspheric element with positive power made of APEL optical polymers, whereas the other is an aspheric element with negative power made of OKP1 optical polymers. As both lenses have a focal length of approximately 2.0 mm with effective aperture of 2.0 mm, the WaveMaster Pro wavefront measurement system is employed for measurement of the LUTs. Figures 9 and 10 show the comparisons of wavefront maps between the measured and the simulated results for both the positive and negative power elements. Moreover, the Zernike coefficients of the wavefront data are tabulated in Table 1 with the corresponding specific physical correlation for process parameters. The results indicate that larger wavefront aberrations, such as astigmatism in convex lenses, may still be significant even though aspheric surfaces have been adopted in the design. This observation confirms the shop-floor empirical results from local communications among production engineers concerning the root cause of
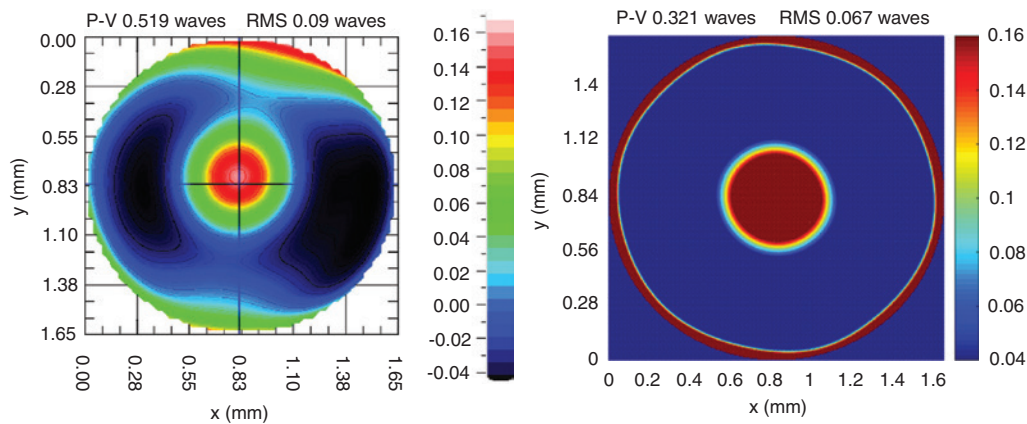

Figure 9: Comparisons of wavefront maps between the measured (left) and the simulated (right) data from the negative power lens element.
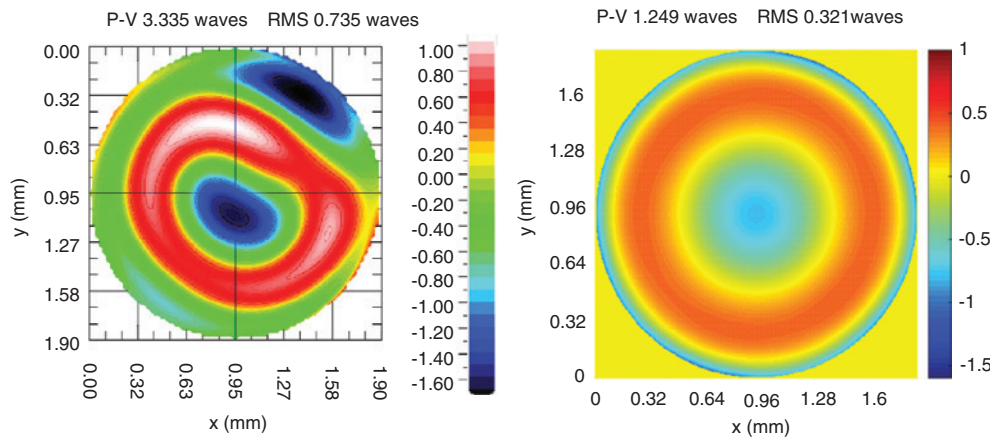
Figure 10: Comparisons of wavefront maps between the measured (left) and the simulated (right) data from the positive power lens element.

Table 1: Comparisons of wavefront aberrations expressed by Zernike polynomial between the simulated and the measured lens elements of a mobile-phone camera.

Zernike coefficient in [n][m]	Concave lens element		Convex lens element	
	Design	**Measured**	**Design**	**Measured**
Defocus [2][0]	-0.034	0.002	-0.002	-0.003
Astigmatism [2][-2]	-0.017	0.054	0.095	-0.314
Astigmatism [2][2]	7.0×10^{-16}	-0.001	-6.0×10^{-5}	0.673
Coma [3][1]	2.2127×10^{-15}	-0.007	6.039×10^{-15}	0.352
Coma [3][-1]	5.0540×10^{-15}	0.007	-2.058×10^{-15}	-0.051
Primary spherical [4][0]	0.0565	-0.084	-3.561	0.651
P-V errors (λ)	0.132	0.326	0.981	2.996
RMS errors (λ)	0.030	0.060	0.240	0.716

difficulty in the production of convex elements of mobile-phone cameras.

5 Conclusions

This paper successfully establishes and verifies the wavefront measurement systems for explaining factors influencing image quality, including surface deviations, refractive index variations, and residual birefringence. Furthermore, if the CAE mold-flow simulation results are available, the wavefront aberrations contributed by injection-molding process parameters can be theoretically identified. Furthermore, optical performance qualities such as PSF, MTF, and Strehl ratio can all be calculated based on the wavefront measurements, though not described and discussed in this paper. More importantly, the wavefront measurement systems based on SHS are readily available for any optical lens with aspheric surfaces if reconfiguration of optics layout is possible. In the future, research work could be focused on the study of compensation in refractive index variations and multiple-lens wavefront aberrations during the lens automatic assembly processes.

References

[1] R. B. Johnson, V. N. Mahajan and S. Thibault, in: 'Proc. of SPIE Vol. 9192 91920H-1' (2014), p. 91920H.
[2] C. H. Tsai and W. Y. Chen, Optical lens assembly for image taking, US Patent 2014/0327975 A1.
[3] T. Steinich and V. Blahnik, Adv. Opt. Techn. 1, 51–58 (2012).

[4] W. Michaeli, S. Hessner, F. Klaiber and J. Forster, CIRP Ann-Manuf. Tech. 56, 545–548 (2007).

[5] C. Yang, L. Su, C. Huang, H. X. Huang, J. Castro, et al. Adv. Polym. Tech 30, 51–61 (2011).

[6] L. Li, T. W. Raasch and A. Y. Yi, Appl. Optics 24, 6022–6029 (2013).

[7] J. C. Wyant and K. Creath, Appl. Optics Optical Eng. 11, 2–34 (1992).

[8] D. R. Neal, D. J. Armstrong and W. T. Turner, Lasers as Tools for Manufacturing II, SPIE vol. 2993 (1997).

[9] H. Liu, Z. Lu and F. Li, Optics Laser Tech. 37, 642–646 (2005).

[10] F. Merola, M. Paturzo, S. Coppola, V. Vespini and P. Ferraro, J. Micromech. Microeng. 19, 125006 (2009).

[11] R. R. Rammage, D. R. Neal and R. J. Copland, in 'Application of Shack-Hartmann Wavefront Sensing Technology to Transmissive Optic Metrology' Adv. Characterization Tech. for Optical, Semiconductor, and Data Storage Comp., SPIE Vol. 4779, (2002).

[12] Wavefront sensors, Available at: http://www.trioptics.com/products/wavefront-sensors/, Germany (2016), Accessed 12 April, 2016.

[13] D. Malacara, in 'Optical Shop Testing, 3rd ed.' (John-Wiley and Sons Inc., New York, 2007, Chapters 10–12), pp. 362–497.

[14] L. Li, T. W. Raasch, I. Sieber, E. Beckert, R. Steinkopf, et al. Appl. Optics 19, 4248–4255 (2014).

[15] T. Higashihara and M. Ueda, Macromolecules 48, 1915–1929 (2015).